Atmos. Meas. Tech. Discuss., 3, 2367–2387, 2010
www.atmos-meas-tech-discuss.net/3/2367/2010/
doi:10.5194/amtd-3-2367-2010

Atmospheric Measurement Techniques Discussions

Columnar aerosol size distribution function obtained by inversion of spectral optical depth measurements for the Zanjan, Iran

A. Masoumi, A. Bayat, and H. R. Khalesifard

Institute for Advanced Studies in Basic Sciences (IASBS), P.O. Box 45195-1159, Zanjan, 45195, Iran

Received: 26 April 2010 – Accepted: 19 May 2010 – Published: 28 May 2010

Correspondence to: A. Masoumi (masoumi@iasbs.ac.ir)

Published by Copernicus Publications on behalf of the European Geosciences Union.

Abstract

We are reporting the calculated values of columnar aerosol size distribution function for atmosphere of Zanjan, a city in Northwest Iran (36.70° N, 48.51° E). Ground-based measurements of the total optical depth of the Zanjan atmosphere at 440 nm, 670 nm, 870 nm, and 1020 nm are recorded using a Cimel CE318-2 sunphotometer in the period of October 2006 to September 2008. The spectral aerosol optical depth has been obtained by subtraction of molecular optical depth from the total optical depth for each wavelength channel. Also the Ångström exponent is determined by a logarithmic fit to the aerosol optical depth when it is plotted versus the logarithm of the wavelength. Daily averages of the measured aerosol optical depth and Ångström exponent values have been implemented in an inversion algorithm for calculation of the columnar aerosol size distribution function. In this algorithm, the aerosols are considered as spheres of different size and refractive index of 1.45. We found that for 82% of the days, aerosols are in the coarse mode. For these days, more than 50% of the aerosol volume concentration has a radius >1 µm. We believe this is related to the geographical location of Zanjan in a mostly dry area and subject to frequent dust winds.

1 Introduction

Zanjan, a city in Northwest Iran located at 36.70° N, 48.51° E and 1800 m above the mean sea level, frequently experiences dust storms in the spring and summer. Dust sources like the Tigris and Euphrates basin have a major role in the aerosol content of this region (Prospero et al., 2002). Other resources like the anthropogenic aerosols and dust from Qom Lake are other minor contaminants in the atmosphere of this area (Mortazavy, 2009). Here we are reporting the size distribution for aerosols for this area that has been calculated by an inversion algorithm applied to the aerosol optical depth (AOD) recorded during October 2006 to September 2008. The AOD values have been

AMTD
3, 2367–2387, 2010

retrieved from the data recorded by a Cimel CE318-2 sunphotometer (SPM) in the sun mode (Holben et al., 1998).

Aerosol particles affect the climate system via direct and indirect mechanisms. They scatter and absorb both solar and thermal radiations and change cloud characteristics in many ways (Haywood and Boucher, 2000; Lohmann and Feichter, 2005). Size distribution together with other optical and microphysical properties of aerosols are important in assessment of such effects (Wang et al., 2006; Romanov et al., 1999). So it is necessary to determine the size distribution function of the aerosols, $n(r)$, in a mathematical formalism. The relationship between the size of atmospheric aerosols and the wavelength-dependent extinction coefficient was first suggested by Ångström in 1929 (Angstrom, 1929). Since then the size distribution began to be retrieved by extinction measurements (Wang et al., 2006). In 1969 Yamamoto and Tanaka were the first to apply a numerical inversion algorithm to spectral measurements of extinction coefficient in order to determine an aerosol size distribution (King et al., 1978; Yamamoto and Tanaka, 1969). We use the same method to determine $n(r)$ for the aerosols in the atmosphere of Zanjan in the mentioned time period. Our results show for 82% of the days, supermicron aerosols (aerosols with radius >1 μm) constitute the largest fraction of the aerosol volume concentration and for the rest of the days, submicron aerosols (aerosols with radius <1 μm) are dominant.

2 Method

The attenuation of solar radiation passing through the atmosphere is given by Bouguer-Beer-Lambert law,

$$I_\lambda = I_{0\lambda}\, \mathrm{e}^{-m\tau_{\mathrm{tot},\lambda}}, \tag{1}$$

Where I_λ is the observed spectral direct-beam irradiance at wavelength λ, $I_{0\lambda}$ is the extraterrestrial solar spectrum corrected for the actual sun-earth distance, m is the optical air mass and $\tau_{\mathrm{tot},\lambda}$ is the wavelength-dependent total optical depth (TOD) (Kaskaoutis

AMTD
3, 2367–2387, 2010

et al., 2006). TOD for each recording of the SPM in the sun mode can be calculated from Eq. (1). After subtracting the mean daily molecular optical depth (MOD) from the daily-averaged TOD, the aerosol optical depth (AOD) will be obtained (Bodhaine et al., 1999). The AOD or $\tau_{a,\lambda}$, like TOD is calculated for four wavelengths, 440 nm, 670 nm, 870 nm, and 1020 nm. Ångström empirical formula is written as,

$$\tau_{a,\lambda} = \beta\, \lambda^{-\alpha}, \tag{2}$$

Where β is the turbidity coefficient and α is the Ångström exponent reflecting the aerosol size distribution (Wang et al., 2006). The Ångström exponent is determined by a logarithmic fit to the AOD when it is plotted versus the logarithm of the wavelength. The obtained AODs at three wavelength channels, 440 nm, 670 nm, and 870 nm have been used to retrieve α (Kaskaoutis et al., 2007). Assuming a spherical shape and refractive index of m' for the aerosols, the AOD and aerosol size distribution function relate as,

$$\tau_{a,\lambda} = \int_{r=r_{min}}^{r=r_{max}} \int_{z=0}^{z=\infty} \pi\, r^2 Q_{ext}(r,\lambda,m') n'(r,z) dz dr, \tag{3}$$

Where $n'(r,z)$ is the height-dependent aerosol number density in the radius range r to $r+dr$; and $Q_{ext}(r,\lambda,m')$ the extinction efficiency factor from the Mie theory (King et al., 1978). Since all measured quantities by the SPM are summed over the atmospheric column, we replace $n'(r,z)$ with,

$$n(r) = \int_{z=0}^{z=\infty} n'(r,z) dz, \tag{4}$$

Where $n(r)$ is the unknown columnar aerosol size distribution, i.e., the number of particles per unit of area per the unit radius interval, in a vertical column through the atmosphere (King et al., 1978). Considering Eq. (4), Eq. (3) can be written as,

$$\tau_{a,\lambda} = \int_{r_{min}}^{r_{max}} \pi\, r^2 Q_{ext}(r,\lambda,m') n(r) dr. \tag{5}$$

AMTD
3, 2367–2387, 2010

One can retrieve the aerosol size distribution by inversion of the AOD measurements through Eq. (5) (King et al., 1978). In this work, the aerosols are considered as spheres of different size from r_{min}=5 nm to r_{max}=2 µm and refractive index of m'=1.45. In order to find the exact value of $n(r)$, a continuous spectra of $\tau_{a,\lambda}$ is needed, when the SPM measurements are in the sun mode. In other words the AOD should be measured in a wide spectral region (e.g. Vis-NIR) when the number of measurements is determined by dividing the length of the spectral region to the band width of the SPM filters. This will gives quite a large number of equations like Eq. (5). But we are measuring the AOD only on four wavelength channels. So we can determine $n(r)$ only for four radius values. In other words we will solve Eq. (5) for four specified radius intervals, when each interval will be represented by its midpoint. Therefore Eq. (5) can be written as,

$$\tau_{a,\lambda} = \sum_{j=1}^{4} \int_{r_j}^{r_{j+1}} \pi\, r^2 Q_{ext}(r,\lambda,m') n(r) dr, \tag{6}$$

When the integration limits are r_1=r_{min}=5 nm, r_2=0.5 µm, r_3=1 µm, r_4=1.5 µm, and r_5=r_{max}=2 µm. We let $n(r)$=$h(r)f(r)$, when $h(r)$ is a rapid varying function of r and $f(r)$ is more slowly varying. A Junge size distribution can be considered for $h(r)$ (King et al., 1978),

$$h(r) = r^{-(\alpha+3)}. \tag{7}$$

We consider all the particles with radii in the range of r_j to r_{j+1} to have the same $f(r)$=f_j and Eq. (6) becomes,

$$\tau_{a,\lambda} = \sum_{j=1}^{4} f_j \int_{r_j}^{r_{j+1}} \pi\, r^2 Q_{ext}(r,\lambda,m') r^{-(\alpha+3)} dr. \tag{8}$$

Considering the four mentioned wavelengths, Eq. (8) can be written as a matrix equation,

$$\mathbf{T} = \mathbf{A}\,\mathbf{F} + \epsilon. \tag{9}$$

AMTD
3, 2367–2387, 2010

T is a columnar matrix whose elements are $T_i=\tau_{a,\lambda_i}$, i=1,2,3,4, and representing the AOD value at λ_i. **F** is a columnar matrix and its elements are, $F_j=f(\bar{r}_j)$, j=1,2,3,4, and $\bar{r}_j=(r_j+r_{j+1})/2$ is the midpoint of r_j and r_{j+1}. **A** is a square matrix and its elements are representing by, $A_{ij}=\int_{r_j}^{r_{j+1}}\pi r^2 Q_{ext}(r,\lambda_i,m')r^{-(\alpha+3)}dr$, and ϵ is an unknown error vector whose elements ϵ_i represent the deviation between measured AODs (T_i) and their theoretical values ($\sum_{j=1}^{4}A_{ij}F_j$) (King et al., 1978). The conventional approach to such a problem is to use the least square techniques and then Eq. (9) can be written as,

$$\mathbf{F} = (\mathbf{A}^{\mathbf{T}}\mathbf{A})^{-1}\mathbf{A}^{\mathbf{T}}\mathbf{T}, \tag{10}$$

Where $\mathbf{A}^{\mathbf{T}}$ is transpose of **A** (Liou, 2002). The constrained linear inversion solution to solve this problem has the following form (Liou, 2002),

$$\mathbf{F} = (\mathbf{A}^{\mathbf{T}}\mathbf{A} + \gamma\mathbf{H})^{-1}\mathbf{A}^{\mathbf{T}}\mathbf{T}, \tag{11}$$

Where **H** is a ($N\times N$) matrix given by,

$$\mathbf{H} = \begin{pmatrix} 1-N^{-1} & -N^{-1} & \dots & -N^{-1} \\ -N^{-1} & 1-N^{-1} & \dots & -N^{-1} \\ \vdots & \vdots & & \vdots \\ -N^{-1} & -N^{-1} & \dots & 1-N^{-1} \end{pmatrix}. \tag{12}$$

N is the number of wavelengths used in the measurements (for our case N=4), and γ is a non-negative multiplier (Liou, 2002). In performing the inversion described above, it is necessary to select a value for γ, but referring to Eq. (11), $\gamma_{rel}=(\gamma\mathbf{H})_{11}/(\mathbf{A}^{\mathbf{T}}\mathbf{A})_{11}$ is the dominant term (King et al., 1978). A minimum value for γ_{rel} should be chosen in a way that all elements of **F** are positive (negative values are not physical solution). γ_{rel} is allowed to vary in the range 10^{-3} to 1 (King et al., 1978). As we calculated it for our data we found that its most probable value is $\sim 10^{-2}$ in our measurements. Knowing the elements of the matrix **F** from Eq. (11), one can write a discrete aerosol size distribution as,

$$n(\bar{r}_j) = (\bar{r}_j)^{-(\alpha+3)}F_j. \tag{13}$$

AMTD
3, 2367–2387, 2010

3 Aerosol size distribution results

The method described in the previous section has been applied to the recorded data by our SPM during October 2006 to September 2008. We chose 97 sunny days of this period. The values of $n(r)$ have been determined for the midpoints of the coarse radius intervals, $\bar{r}_1$=0.25 µm, $\bar{r}_2$=0.75 µm, $\bar{r}_3$=1.25 µm, and $\bar{r}_4$=1.75 µm. These are representative of very fine, fine, coarse, and very coarse aerosols respectively. So we are defining four classes of aerosol sizes. As it appeared in Fig. 1, even though always the number of very fine aerosols is more than other aerosol sizes, but for 82% of the days, number of coarse aerosols is more than fine ones and for these days α<1.2. For rest of the days, number of fine aerosols is more than coarse aerosols and $\alpha \geq 1.2$. Also for about 10% of the days, amount of very coarse aerosols is considerable and number of them is more than half of coarse aerosols. For such days α has values smaller than 0.2. We entitled Fine, Coarse, and Very Coarse for these situations respectively (Very Coarse-mode is a subset of Coarse-mode). Figure 1 shows the average size distribution of the aerosols for the whole data set (i.e. 97 days). In Fig. 1 average size distribution of the Coarse-mode days labeled as a Coarse, average size distribution of the Fine-mode days labeled as a Fine, and finally average size distribution of the days including very coarse aerosols are in the same order (>50%) as the coarse aerosols labeled as a Very Coarse.

Referring to Eq. (13), the value of α determines relative population of aerosols in the four mentioned classes of aerosol sizes. In other words for a specific value of α the aerosol size distributions show similar behavior even though the AOD values for the measurements are different. Figure 2 shows the aerosol size distribution for 6 June 2007, 8 October 2007, and 18 October 2006 when α has a constant value of ~0.71, but the AOD has different values of 0.11, 0.27, and 0.41 at 440 nm respectively. It can be seen in Fig. 2 that the aerosol size distributions for these three days have almost the same behavior. On the other hand when the AOD for two other days, 4 July 2008, and 6 May 2007 is almost constant (~0.36) but the values of α are 0.09,

AMTD
3, 2367–2387, 2010

and 0.22 respectively, the aerosol size distribution functions show different behavior (Fig. 3). The calculated values of total aerosol volume concentrations are the same for these two days (~0.13 $\mu m^3/\mu m^2$). In other words the AOD represents the total volume concentrations of the aerosols present in the atmosphere.

4 Discussion

Since Zanjan is located in an arid area, its atmosphere mostly is not subjected to the aerosols of marine origin and biomass burning aerosols. Therefore we can divide aerosol types for Zanjan into urban-industrial and desert dust aerosols (Dubovik et al., 2002). We now discuss each of these two aerosol types of Zanjan atmosphere separately.

4.1 Urban-industrial aerosol

Our 2-year SPM data shows that for 18% of the days, aerosols with radius <1 μm have more than 50% of the aerosol volume concentrations. For these days, the number of fine-mode aerosols is higher than the number of coarse aerosols and $\alpha \geq 1.2$. These situations usually happen on December, January and February. Figure 4 shows the aerosol size distribution function for one of such days (25 December 2006). Figure 5 is output of NOAA ARL (Aerosol Resource Laboratory) HYSPLIT model for this day (Draxler and Rolph, 2010; Rolph, 2010). In this figure the back-trajectories ending at 10:00 UTC and duration of 48 hours, on December 25, 2006 at three different altitudes 500 m, 1500 m, and 2500 m a.g.l. (above ground level) are plotted for Zanjan area. Of course the continental Europe is not a dust source for this region. On the other hand Zanjan often covered by snow at the end of autumn and winter and it could not have noticeable local dust. So we expect that the local urban anthropogenic aerosols of Zanjan have a considerable share in the aerosol content for this day. It is in agreement

AMTD
3, 2367–2387, 2010

with aerosol size distribution results of such days. So we often have aerosols of fine mode and minimum value of AOD for similar situations on December, January and February.

4.2 Desert dust aerosol

For 82% of the days, aerosols with radius >1 µm have more than 50% of the aerosol volume concentrations. For these days, the number of coarse aerosols is more than fine aerosols and we have $\alpha \leq 1.2$. We believe this related to Zanjan geographical location when it is located in a dry area and subjected to frequent dust winds. Dust sources like Tigris and Euphrates basin has a major role in the aerosol content of this region (Prospero et al., 2002). Other resources like the dust from Qom Lake and environs of Zanjan are other minor contaminants in the atmosphere of this area (Mortazavy, 2009). We see such days in the whole of the year specially at the spring and beginning of the summer on April, May, June and July. As an example, aerosol size distribution function for 4 July 2008 is shown in the Fig. 6. Figure 7 is the output of NOAA ARL (Aerosol Resource Laboratory) HYSPLIT model for this day (Draxler and Rolph, 2010; Rolph, 2010). HYSPLIT model results for this day show that air parcels are coming from Iraq at three different altitudes 500 m, 1500 m, and 2500 m a.g.l. It means that dust from Tigris and Euphrates basin is loaded into the air parcels and transferred to the atmosphere of Zanjan. Therefore the number of coarse and very coarse aerosols is dominant in the atmosphere. As reported by the Zanjan Met. Office during 3 July afternoon to 4 July 2008 morning the visibility was reduced to less than 8 km. These two reasons, i.e., the result of NOAA ARL HYSPLIT model, back-trajectories and report of the atmospheric visibility of Zanjan Met. Office, are in agreement with aerosol size distribution results of 4 July 2008 (see Fig. 6). So we often have aerosols of coarse mode and maximum value of AOD for similar situations in the whole of the year specially on April, May, June and July.

AMTD
3, 2367–2387, 2010

5 Conclusions

We summarized monthly-averages of some of aerosol properties such as submicron and supermicron volume concentrations, α, and AOD (440 nm) values in Table 1. Table 1 shows that the aerosols of fine mode mostly are dominant on December and January while AOD reaches to its minimum values. So we can say that the aerosols of these two months belong to the urban-industrial type. On the other hand we see the maximum supermicron aerosols volume concentration in the spring and beginning of the summer. We relate the maximum value of the AOD and noticeable increase of very coarse aerosols during this period to the transfer of dust from source regions like the Tigris and Euphrates basin. Finally, we see a mixture of urban-industrial and dust aerosols during must of the year. The AOD values are maximum when the Ångström exponent is indicative of supermicron aerosols (during spring and summer) and are minimum when α has its largest values (December and January) indicating for an atmosphere mostly loaded with fine and very fine aerosols. Figure 8 depicts the seasonal averages of aerosol size distribution function. As it can be seen in Fig. 8, the number of fine and very fine aerosols are almost constant during different seasons of the year but coarse and very coarse aerosols are considerably increasing during spring and summer. Aerosols of autumn and winter seasons are in the fine mode and behavior of the aerosol size distributions of these two seasons are the same; although the number of aerosols in winter is slightly less than those in autumn for all sizes. We relate that to the existence of mixture of urban-industrial and dust aerosols with dominant share of urban-industrial type especially in the winter. On the other hand we see that the aerosols of spring and summer times are in the coarse mode and have the same behavior. We can relate the increase of number of coarse and very coarse aerosols in spring and summer times to the increase of dust aerosols in the atmosphere. This can be due to transfer of dust aerosols from the sources like Tigris and Euphrates basin and Qom Lake to Zanjan atmosphere.

AMTD
3, 2367–2387, 2010

Acknowledgements. The authors would like to express their gratitude to Farhad Abdi for valuable discussions. They also would like to acknowledge the Zanjan Met. Office for providing the Zanjan atmosphere visibility data and gratefully acknowledge the NOAA Air Resources Laboratory (ARL) for the provision of the HYSPLIT transport and dispersion model and/or READY website (http://www.arl.noaa.gov/ready.php) used in this publication.

References

Angstrom, A.: On the atmospheric transmission of sun radiation and on dust in the air, Geogr. Ann., 11, 156–166, 1929. 2369

Bodhaine, B. A., Wood, N. B., Dutton, E. G., and Slusser, J. R.: On Rayleigh optical depth calculations, J. Atmos. Ocean. Tech., 16, 1854–1861, 1999. 2370

Draxler, R. R. and Rolph, G. D.: HYSPLIT (HYbrid Single-Particle Lagrangian Integrated Trajectory) Model access via NOAA ARL READY Website: http://ready.arl.noaa.gov/HYSPLIT.php, last access: 27 May 2010, NOAA Air Resources Laboratory, Silver Spring, MD, 2010. 2374, 2375

Dubovik, O., Holben, B. N., Eck, T. F., Smirnov, A., Kaufman, Y. J., King, M. D., Tanre, D., and Slutsker, I.: Variability of absorption and optical properties of key aerosol types observed in worldwide locations, J. Atmos. Sci., 59, 590–608, 2002. 2374

Haywood, J. M. and Boucher, O.: Estimates of the direct and indirect radiative forcing due to tropospheric aerosols: a review, Rev. Geophys., 38, 513–543, 2000. 2369

Holben, B. N., Eck, T. F., Slutsker, I., Tanre, D., Buis, J. P., Setzer, A., Vermote, E., Reagan, J. A., Kaufman, Y. J., Nakajima, T., Lavenu, F., Jankowiak, I., and Smirnov, A.: AERONET-A federated instrument network and data archive for aerosol characterization, Remote Sens. Environ., 66, 1–16, doi:10.1016/S0034-4257(98)00031-5, 1998. 2369

Kaskaoutis, D. G., Kambezidis, H. D., Adamopoulos, A. D., and Kassomenos, P. A.: Comparison between experimental data and modelling estimates of aerosol optical depth over Athens, Greece, J. Atmos. Sol.-Terr. Phy., 68, 1167–1178, doi:10.1016/j.jastp.2006.02.011, 2006. 2369

AMTD

3, 2367–2387, 2010

Kaskaoutis, D. G., Kambezidis, H. D., Hatzianastassiou, N., Kosmopoulos, P. G., and Badarinath, K. V. S.: Aerosol climatology: dependence of the Angstrom exponent on wavelength over four AERONET sites, Atmos. Chem. Phys. Discuss., 7, 7347–7397, doi:10.5194/acpd-7-7347-2007, 2007. 2370

King, M. D., Byrne, D. M., Herman, B. M., and Reagan, J. A.: Aerosol size distributions obtained by inversion of spectral optical depth measurements, J. Atmos. Sci., 35, 2153–2167, doi:10.1175/1520-0469(1978)035<2153:ASDOBI>2.0.CO;2, 1978. 2369, 2370, 2371, 2372

Liou, K. N.: An Introduction to Atmospheric Radiation, in: International Geophysics Series, Second Edition, Vol. 84, edited by: Dmowska, R., Holton, J. R., and Rossby, H. T., Academic Press, USA, 2002. 2372

Lohmann, U. and Feichter, J.: Global indirect aerosol effects: a review, Atmos. Chem. Phys., 5, 715–737, doi:10.5194/acp-5-715-2005, 2005. 2369

Mortazavy, F.: Characterizing the resources and type of aerosols in the Zanjan atmosphere using the data recorded by a sunphotometer, Hysplit4 and Giovanni models, M. Sc. Thesis, IASBS, Zanjan, Iran, 2009. 2368, 2375

Prospero, J. M., Ginoux, P., Torres, O., Nicholson, S. E., and Gill, T. E.: Environmental characterization of global sources of atmospheric soil dust identified with the Nimbus 7 total ozone mapping spectrometer (TOMS) absorbing aerosol product, Rev. Geophys., 40(1), 1002, doi:10.1029/2000RG000095, 2002. 2368, 2375

Rolph, G. D.: Real-time Environmental Applications and Display sYstem (READY) Website: http://ready.arl.noaa.gov, last access: 27 May 2010, NOAA Air Resources Laboratory, Silver Spring, MD, 2010. 2374, 2375

Romanov, P., O'Neill, N. T., Royer, A., and McArthur, B. L. J.: Simultaneous retrieval of aerosol refractive index and particle size distribution from ground-based measurements of direct and scattered solar radiation, Appl. Optics, 38, 7305–7320, 1999. 2369

Wang, Y., Fan, S., Feng, X., Yan, G., and Guan, Y.: Regularized inversion method for retrieval of aerosol particle size distribution function in W space, Appl. Optics, 45, 7456–7467, 2006. 2369, 2370

Yamamoto, G. and Tanaka, M.: Determination of aerosol size distribution from spectral attenuation measurements, Appl. Optics, 8, 447–453, 1969. 2369

AMTD
3, 2367–2387, 2010

Table 1. Monthly-averaged aerosol properties of Zanjan's atmosphere derived from sun mode data.

Month	Jan	Feb	Mar	Apr	May	Jun	Jul	Aug	Sep	Oct	Nov	Dec
Submicron Aerosols Volume Concentration (%)	58	34	34	23	20	26	28	35	32	44	43	60
Supermicron Aerosols Volume Concentration (%)	42	66	66	77	80	74	72	65	68	56	57	40
Fine Mode	✓											✓
Coarse Mode		✓	✓	✓	✓	✓	✓	✓	✓	✓	✓	
Ångström Exponent	1.27	0.77	0.65	0.36	0.28	0.41	0.45	0.65	0.60	0.85	0.86	1.28
AOD (440 nm)	0.07	0.10	0.12	0.19	0.18	0.21	0.25	0.26	0.14	0.19	0.15	0.09

AMTD
3, 2367–2387, 2010

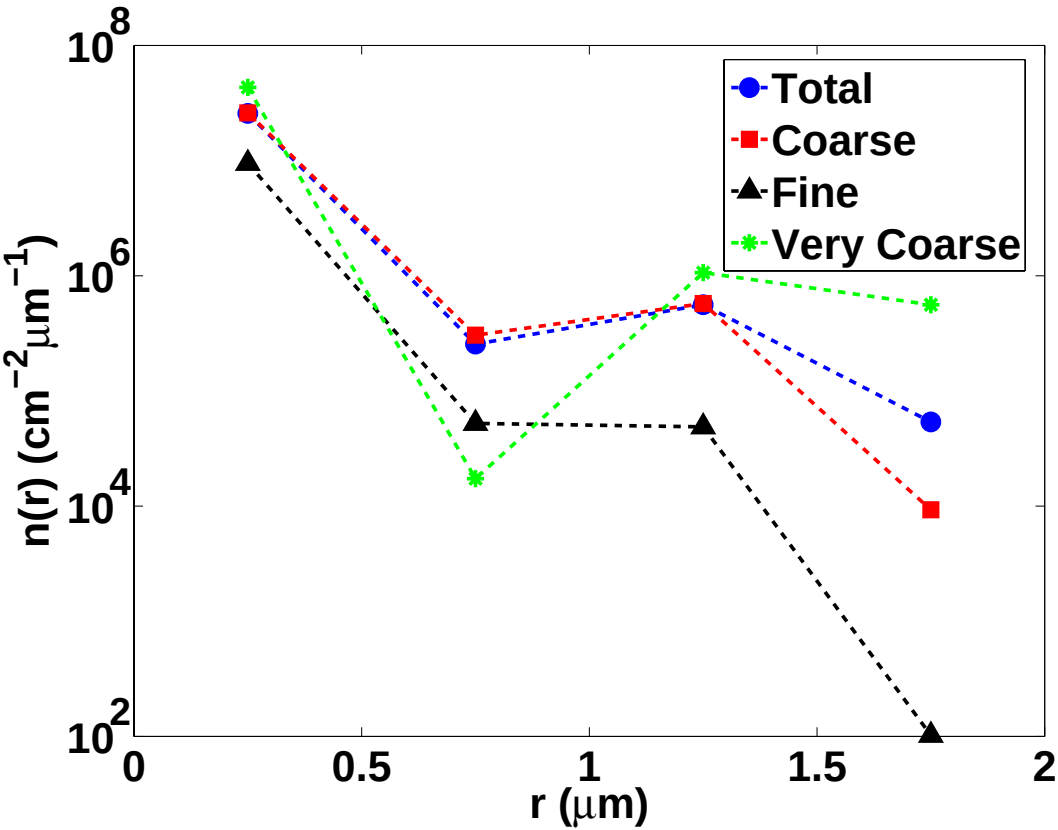

Fig. 1. Average aerosol size distribution function for the whole 97 days (Total), for 80 days (82%) when number of coarse aerosols is greater than fine ones (Coarse), for 17 days (18%) when number of fine aerosols is larger than coarse ones (Fine), and finally for 9 days (10%) when number of very coarse particles is in the same order (>50%) as the coarse aerosols (Very Coarse).

AMTD
3, 2367–2387, 2010

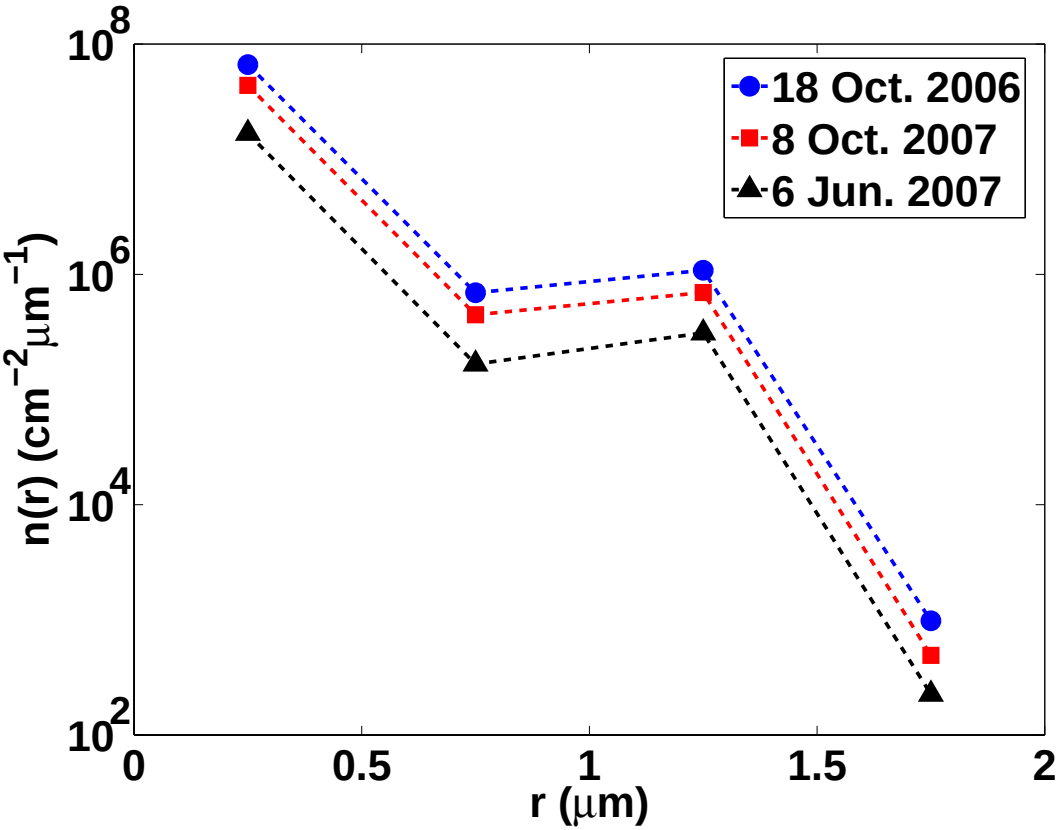

Fig. 2. Aerosol size distributions for 6 June 2007, 8 October 2007, and 18 October 2006 with α=0.71, τ_a (440 nm)=0.11, 0.27, and 0.41 respectively.

AMTD
3, 2367–2387, 2010

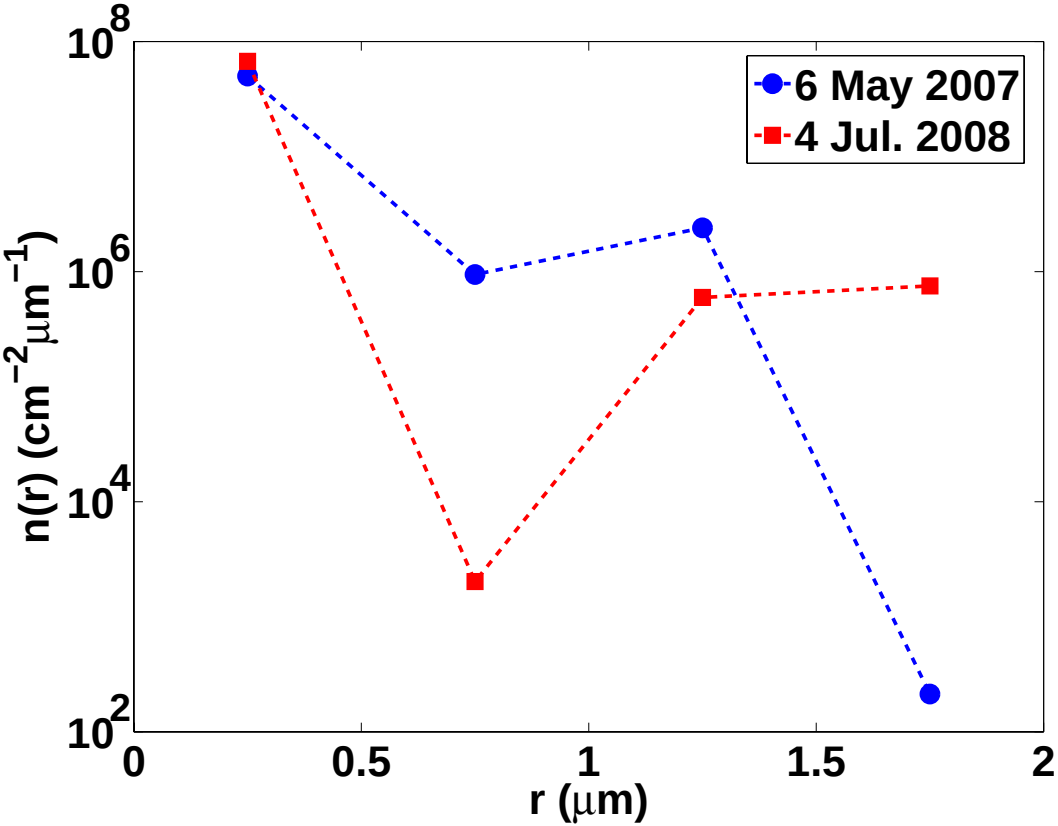

Fig. 3. Aerosol size distributions for 4 July 2008, and 6 May 2007, when τ_a (440 nm)=0.36, for both days and α=0.09, and 0.22 respectively.

AMTD
3, 2367–2387, 2010

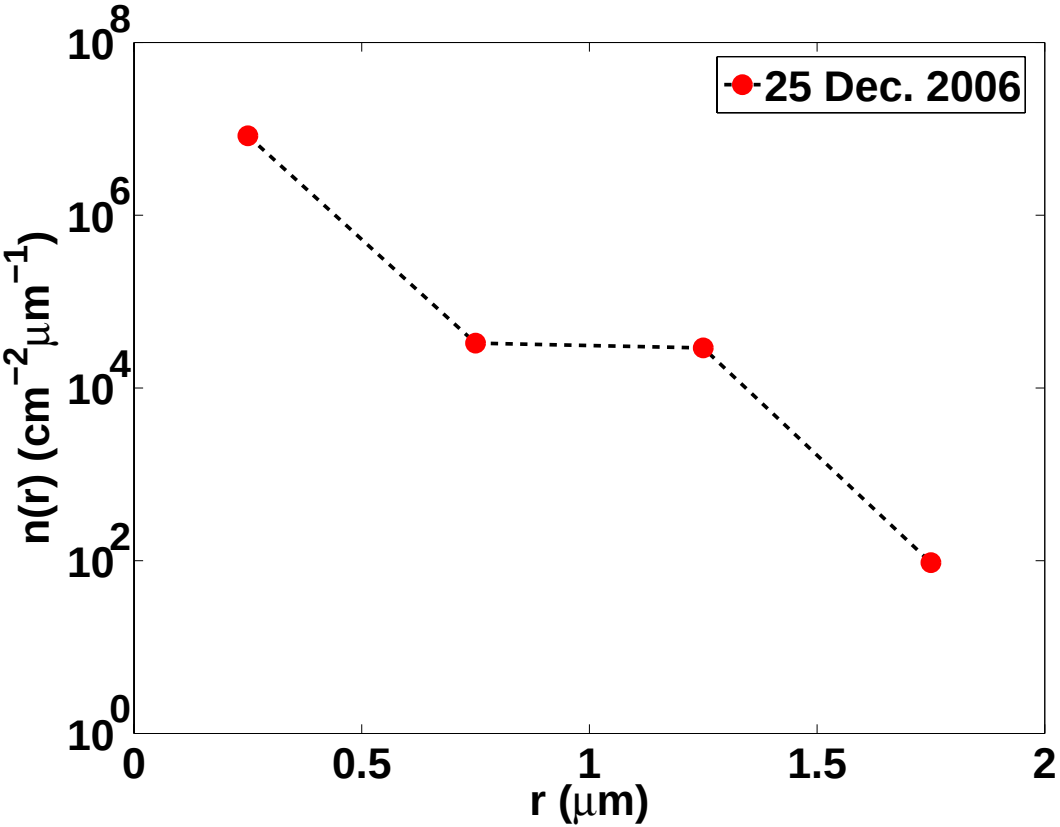

Fig. 4. Aerosol size distribution on 25 December 2006, (α=1.52, τ_a – 440 nm=0.06).

AMTD
3, 2367–2387, 2010

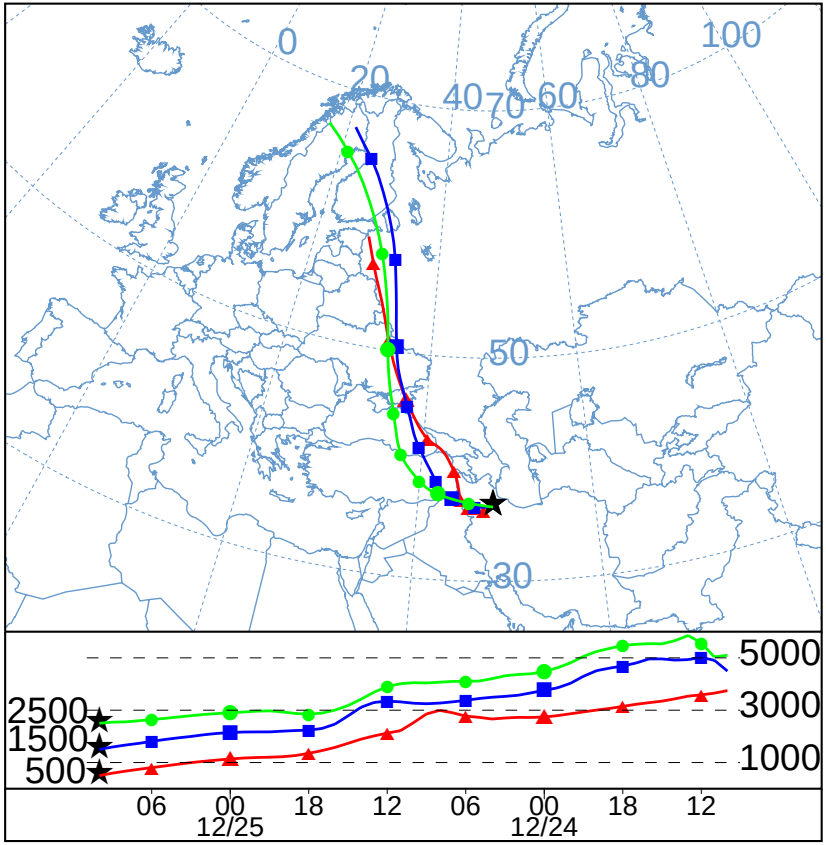

Fig. 5. NOAA ARL HYSPLIT model, back-trajectories calculated for source point at Zanjan (36.70° N, 48.51° E) for 25 December 2006. Vertical motion calculations performed under vertical velocity model for time duration 48 h with ending time 10:00 UTC for altitudes 500 m, 1500 m, and 2500 m a.g.l.

AMTD
3, 2367–2387, 2010

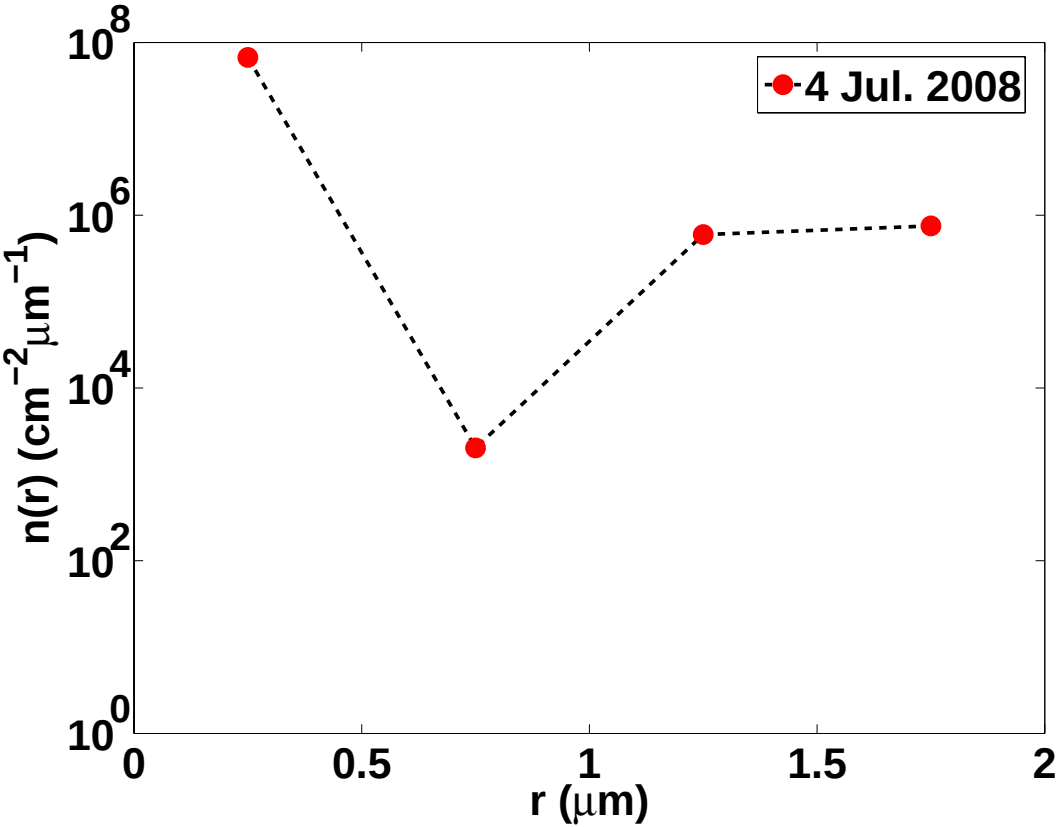

Fig. 6. Aerosol size distribution on 4 July 2008, (α=0.09, τ_a – 440 nm=0.36).

AMTD
3, 2367–2387, 2010

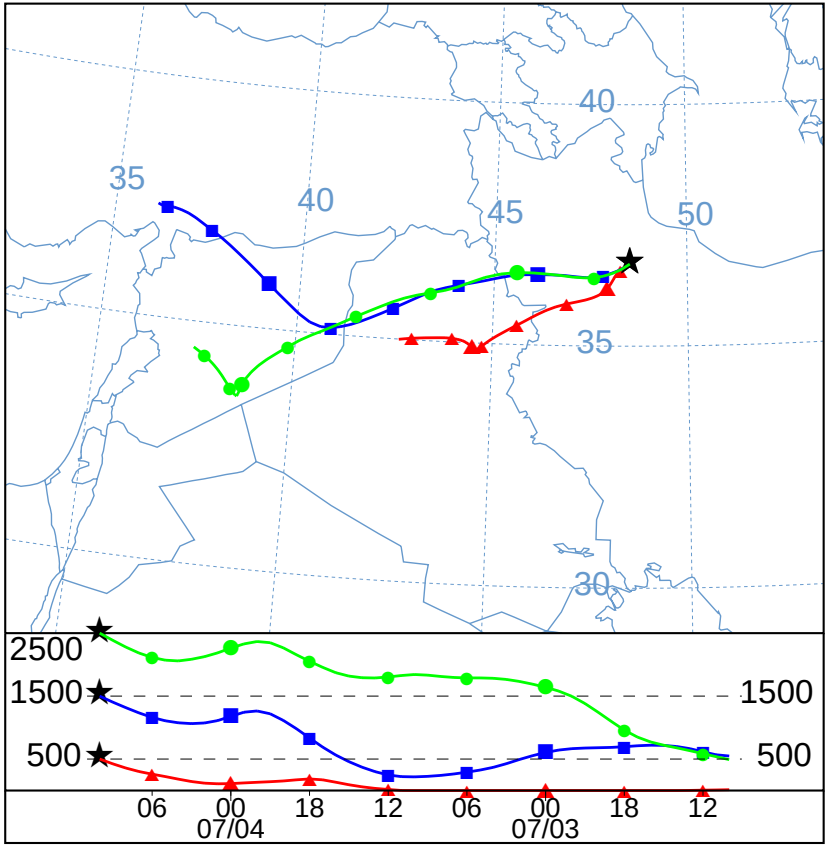

Fig. 7. NOAA ARL HYSPLIT model, back-trajectories calculated for source point at Zanjan (36.70° N, 48.51° E) for 4 July 2008. Vertical motion calculations performed under vertical velocity model for time duration 48 h with ending time 10:00 UTC for altitudes 500 m, 1500 m, and 2500 m a.g.l.

AMTD
3, 2367–2387, 2010

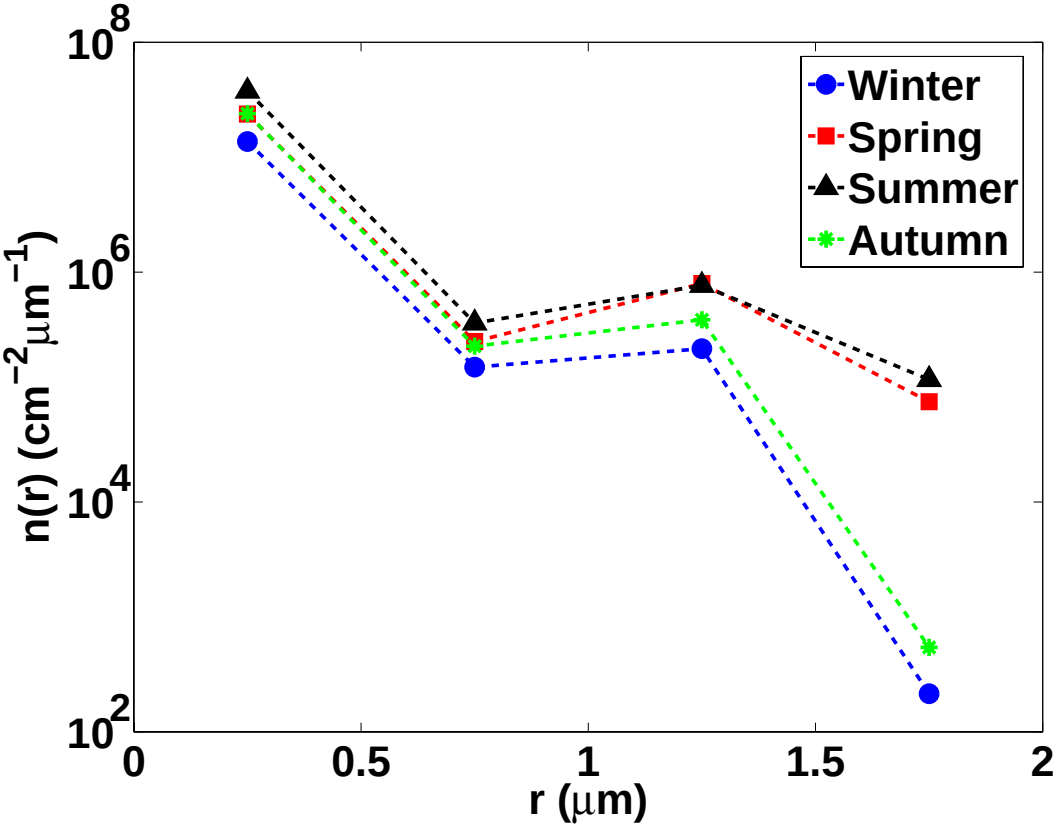

Fig. 8. Seasonal averages of aerosol size distribution function for Zanjan atmosphere.

AMTD
3, 2367–2387, 2010